On the thermal diffusivity of porous silicon

EDVCATIO PHYSICORVM
QVO NON ASCENDAM ?
ISSN 1870-9095

U. Nogal[1], A. Rojas[1], S.A. Salazar-Flores[2], J.C. Sánchez-Nájera[3], L. Luviano[2,a], J. Hernández-Wong[1], M. Aguilar-Frutis[2], J. B. Rojas-Trigos[2], E. Marín[2], A. Calderón[2*]

[1]*SECIHTI-Instituto Politécnico Nacional, CICATA, Unidad Legaria. Legaria No. 694, C.P. 11500 Ciudad de México, México.*
[2]*Instituto Politécnico Nacional. CICATA Unidad Legaria. Legaria 694 Colonia Irrigación, 11500 Ciudad de México, México.*
[3]*Instituto Politécnico Nacional, CECyT 2 Miguel Bernard, Av. Nueva Casa de la Moneda No. 133 Col. Lomas de Sotelo, Del. Miguel Hidalgo, C. P. 11200 Ciudad de México, México.*
[a]Present address: Universidad Tecnológica Fidel Velázquez, Av. Emiliano Zapata S/N, Col. El tráfico, C.P.54474, Nicolás Romero, Estado de México, México.

***E-mail:** jcalderona@ipn.mx

(Received 3 September 2025, accepted 15 December 2025)

Abstract

We report a study investigating the heat-transport capacity of porous n-type silicon samples by examining their effective thermal diffusivity. The effective thermal diffusivity was measured using frequency-domain photoacoustic techniques with a two-layer model that analyzes the thermal resistance of a bilayer system. Porosity was determined through gravimetric methods. The results reveal an almost linear increase in porosity with anodizing time, accompanied by a much greater increase in the thickness of the porous layer. Additionally, we observed a pronounced decrease in effective thermal diffusivity as both porosity and porous layer thickness increased.

Keywords: Porous silicon, electrochemical anodization, thermal diffusivity, photoacoustic.

Resumen

Reportamos un estudio de la capacidad de transporte de calor de muestras de silicio poroso tipo n a través de un estudio de la difusividad térmica efectiva en este material. Los valores medidos de la difusividad térmica efectiva se obtienen mediante la técnica fotoacústica en el dominio de la frecuencia utilizando un modelo de dos capas que se basa en el análisis de la resistencia térmica efectiva de un sistema bicapa, y de la aplicación de la técnica de gravimetría para la determinación de la porosidad. Los resultados muestran un incremento casi lineal de la porosidad con el tiempo de anodización, así como de un incremento mucho mayor del espesor de la capa porosa con el tiempo de anodización. Asimismo, se obtiene un decremento significativo de la difusividad térmica efectiva en dependencia con la porosidad y el espesor de la capa porosa.

Palabras clave: Silicio poroso, anodización electroquímica, difusividad térmica, fotoacústica.

I. INTRODUCTION

For many years, silicon (Si) has been the dominant material in microelectronics. It has the appropriate physical and chemical properties for fabricating microcircuits, is abundant in nature, and is therefore inexpensive. However, Si exhibits poor optical absorption (and even worse optical emission), meaning it cannot efficiently convert electricity into light. This is why optoelectronics has had to rely on gallium arsenide, a more complex and much more expensive semiconductor that can efficiently perform this conversion [1]. In recent years, significant progress has been made in the fabrication of Si-based optoelectronic circuits thanks to the discovery of a very particular form of this material: porous silicon (PSi). Its optical and thermal properties make it a fascinating candidate for applications ranging from sensors to thermal insulation and photonic devices [2, 3, 4, 5, 6, 7, 8, 9, 10]. Understanding how heat transport in this material varies with its structural characteristics is fundamental to unlocking its full potential.

II. POROUS SILICON

Porous silicon (PSi) is a micro- and nano-structured material. As a semiconductor, it is not new; it was discovered accidentally in 1956 by Arthur Uhlir Jr. and his wife, Ingeborg Uhlir, while working at Bell Laboratories in the United States. They observed that under certain electrochemical conditions, Si wafers did not dissolve uniformly as desired, suggesting that electrochemical oxidation preceded chemical oxidation. This was supported by the appearance and behavior of the etched surfaces.

Instead of being shiny, the surfaces had a matte black, brown, or red deposit [11].

The most common and efficient method for producing PSi remains electrochemical etching, also called "anodization," primarily because it allows the desired geometry and architecture to be achieved by varying the current density. PSi is obtained by anodic oxidation of Si in a concentrated hydrofluoric acid (HF) solution. The anode is silicon (Si), and an inert metal such as platinum is used for the cathode. Anodization is generally performed at a constant current density; however, a constant anodizing voltage can also be used. PSi formation depends on the Si doping level and the electrochemical parameters: HF concentration and applied current density [12, 13].

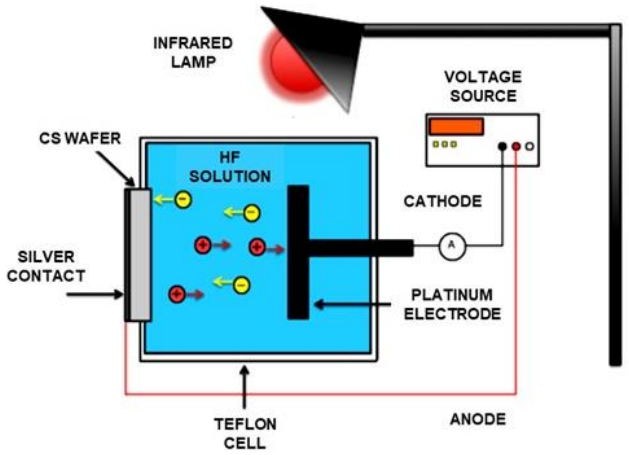

FIGURE 1. Experimental scheme of the anodization process for the elaboration of porous n-type silicon.

Figure 1 shows a simple, typical experimental setup for the fabrication of PSi using the anodization technique. Figure 2 shows images of a sample obtained after 20 minutes of anodization using a current density of 40 mA/cm² and a 40% aqueous HF solution. A phosphorus-doped n-type crystalline silicon (CSi) substrate with a <100> orientation was used in its fabrication. The porous layer has an approximate thickness of 180 μm.

PSi is a system formed by two layers: the porous layer and the substrate. The porous layer is the portion of the sample formed by electrochemical etching of the face in contact with the electrolyte, while the substrate is the portion unaffected by the process. For anodizing times of a few minutes, the porous layer, formed in the CSi, is composed of air cavities surrounded by solid material, whereas for longer anodizing times the porous layer is commonly composed of a thin region (typically about 15-20 μm thick) of material known as the microporous layer, which is responsible for the observed photoluminescence, located above columns of solid material submerged in air, called the macroporous layer, attached to the crystalline silicon (CSi) substrate.

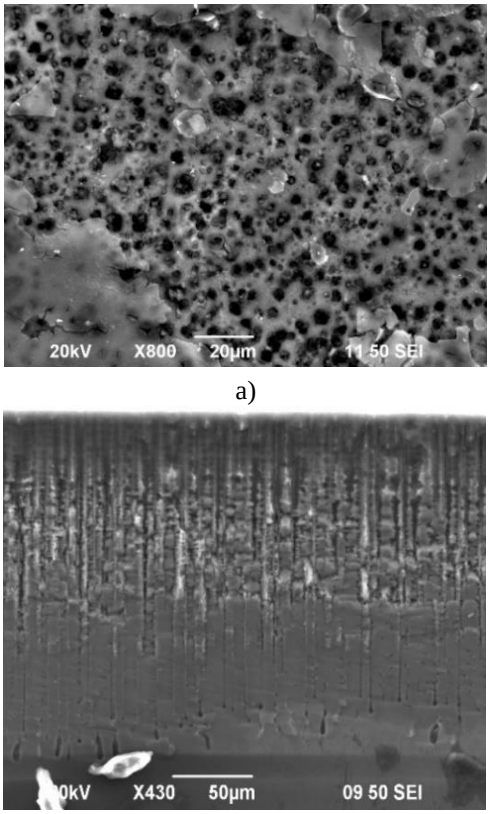

FIGURE 2. a) Surface view and b) side view of a sample of n-type PSi elaborated by anodization. Photographs taken by the authors on a JEOL JSM-6390LV low vacuum SEM at the microscopy laboratory of CICATA-IPN U. Legaria.

III. POROSITY

The porosity (p) of the porous layer is defined as the volume fraction of air in the porous layer and takes values between 0 and 1. It can be shown that, in terms of the mass of the sample before anodization (m_{s_i}), the mass of the entire sample after anodization (m_{s_f}), and the mass of only layer 2 after anodization, the porosity is given as [14]:

$$p = \frac{m_{s_i} - m_{s_f}}{m_{s_i} - m_2}. \quad (1)$$

The determination of porosity using Eq. (4) is known as the gravimetric method, for which porosity measurements with up to 2% accuracy have been reported [15].

IV. EFFECTIVE THERMAL DIFFUSIVITY

It is a material structured into two layers; its thermal properties (thermal conductivity, thermal diffusivity, and heat capacity) are, as a whole, a superposition of the thermal properties of its layers, called effective properties. A direct method for determining these effective properties is to treat

the system as the sum of two thermal resistances in series [16]. Fig. 3 illustrates this situation.

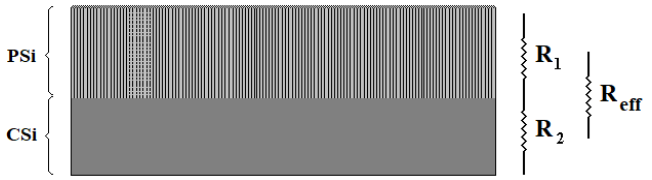

FIGURE 3. Effective thermal resistance of the sum of the thermal resistances of each layer of the Psi.

If l_1, A_1 y k_1 are the thichness, area and termal conductivityof the porous layer, then its termal resistance is given by $R_1 = l_1/A_1\,k_1$, and similarly for the substrate, $R_2 = l_2/A_2\,k_2$. The effective thermal resistance in the perpendicular direction of the two-layer system is expressed as the sum of the thermal resistances of each layer:

$$R_{eff} = \frac{1}{A}\left(\frac{l_1}{k_1} + \frac{l_2}{k_2}\right), \tag{2}$$

where $A = A_1 = A_2$ was defined since both layers have the same surface area.

From the relationship between thermal diffusivity, thermal conductivity, and volumetric specific heat,

$$\alpha = \frac{k}{\rho c}, \tag{3}$$

It can be shown that the effective thermal diffusivity of a two-layer system is given by [17]:

$$\alpha_{eff} = \left(\frac{x^2}{\alpha_1} + \frac{(1-x)^2}{\alpha_2} + x(1-x)\left[\frac{k_1}{k_2\alpha_1} + \frac{k_2}{k_1\alpha_2}\right]\right)^{-1}, \tag{4}$$

where $x = l_1/l$. The last equation implies that the thermal diffusivity of the sample depends not only on the constituent layers' thermal diffusivities but also on the ratio of their thermal conductivities. From this expression, it is possible to obtain the thermal parameters of the porous layer from the corresponding known values of the crystalline silicon substrate [14].

V. MEASURED VALUES

Photoacoustic (PA) technique has proven to be a very useful technique for determining thermal properties in solids.The main reason is because it allows the study of how heat is generated, transported, and dissipated within a material without direct contact, using only intensity-modulated light and the resulting acoustic signal. The PA signal arises from three coupled processes: the absorption of intensity-modulated incident light, the conversion of light to heat, and the generation of acoustic waves [18, 19, 20].

Table I presents the measured effective thermal diffusivity values for porous n-type silicon samples produced by anodizing for times ranging from 10 to 60 minutes. The porous layer thickness fraction and the porosity, measured by the gravimetric method are also included.

TABLE I. Effective thermal diffusivity, anodizing time, and porous layer thickness fraction.

t (*min*)	p	$x = l_1/l$	α_{eff} (cm^2/s)
0	0	0	0.860 ± 0.031
10	0.279	0.083	0.440 ± 0.017
20	0.351	0.408	0.166 ± 0.005
30	0.414	0.554	0.075 ± 0.002
50	0.558	0.748	0.061 ± 0.001
60	0.590	0.816	0.043 ± 0.001

A nearly linear increase in porosity is observed over time, nearly doubling from 10 to 60 minutes of anodizing. In contrast, the relative thickness of the porous layer increases significantly faster over time, increasing almost ninefold from 10 to 60 minutes of anodizing. The increase in porous layer thickness occurs faster than the increase in porosity. Figure 4 illustrates this behavior.

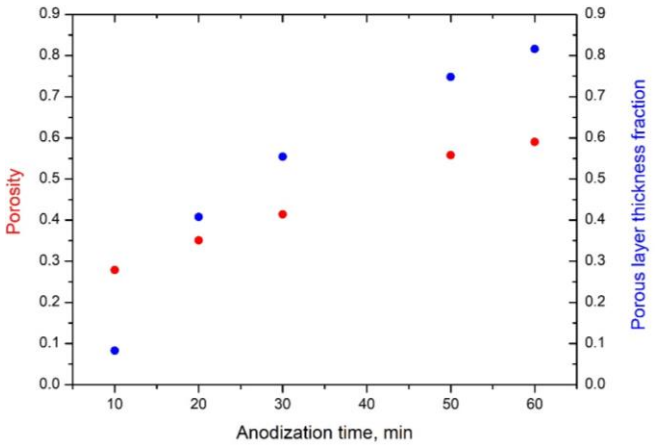

FIGURE 4. Porosity versus anodization time.

Fig. 4 shows the graph of the effective thermal diffusivity as a function of anodizing time. A significant decrease in α_{eff} is observed, dropping from 0.86 cm²/s for CSi to 0.043 cm²/s at a porosity of 59%, representing a 95% decrease from the CSi value.

Thermal diffusivity is the rate at which heat propagates and is damped in the medium [16]. The increase in the thickness and porosity of the porous layer creates a stronger thermal barrier to heat flow, reducing heat transfer capacity and leading to a decrease in effective thermal diffusivity.

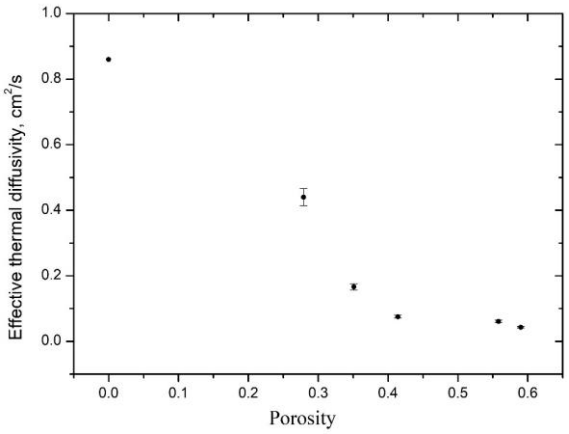

FIGURE 5. Effective termal diffusivity versus porosity.

VI. CONCLUSIONS

Analysis of effective thermal diffusivity shows that variations in porosity and porous layer thickness greatly influence heat transport in this material. Thermal diffusivity, a dynamic parameter associated with time-dependent processes, measures the rate at which heat spreads through a medium. As anodizing time increases, both porous layer thickness and porosity rise, leading to greater thermal resistance and thus a reduced heat transport capacity in porous silicon. These effects are evident in the measured values of effective thermal diffusivity and its dependence on induced porosity and layer thickness.

ACKNOWLEDGMENTS

The authors would like to thank Secretaría de Ciencia, Humanidades, Tecnología e Innovación (SECIHTI), and Secretaría de Investigación y Posgrado (SIP) from Instituto Politécnico Nacional (IPN), both of México for supporting this work through research grants, scholarships to students and incentives to researchers. The support from COFAA-IPN through the SIBE and BEIFI Programs of México is also acknowledged. A. Rojas and L. Luviano thanks from SECIHTI support through Posdoctoral Fellowship.

REFERENCES

[1] Brodsky, M. H., *Gallium arsenide optoelectronic IC's for computer networks*, Superlattives Microstruct **8**, 293-296 (1990).
[2] Sun, X., Sharma, P., Parish, G., Keating, A., *Enabling high-porosity porous silicon as an electronic material*, Micropor. Mesopor. Mat. **312**, 110808 (2021).
[3] Afandi, Y., Parishm, G., Keating, A., *Surface micromachining multilayered porous silicon for spectral filtering applications*, Mater. Sci. Semicond. Process. **138**, 106314 (2022).
[4] James, T., Mannoor, M., Ivanov, D., *BioMEMS – advancing the frontiers of medicine*, Sensors **8**, 6077–6107 (2008).
[5] Canham, L., *Handbook of porous silicon*, (Springer International Publishing, Switzerland, 2020).
[6] Tilli, M. et al., *Hanbook of silicon based MEMS materials and technologies*. Third Ed. Micro and Nano Tech. (Elsevier, 2020), pp. 547-563.
[7] Abd-Elnaiem, A. M., Mohamed, Z. E., Elshahat, S., Almokhtar, M., Norek, M., *Recent progress in the fabrication of photonic crystals based on porous anodic materials*, Energies **16**, 4032 (2023).
[8] Moghimi, E., Azim Araghi, M. E., *Ethanol and Acetone Gas Sensor Properties of Porous Silicon Based on Resistance Response*. *Silicon* **15**, 5821–5827 (2023).
[9] Timoshenko, V. Y., *Porous silicon in photodynamic and photothermal therapy*. Canham, L. Editor, (Springer International Publishing, Switzerland, 2014) pp. 929-936.
[10] Quian, J., Wen, H., Tamarov, K., Xu, W., *Recent developments in Porous Silicon Nanovectors with Various Imaging Modalities in the Framework of Theranostics*, ChemMedChem. **17**, e202200004 (2022).
[11] Uhlir, A., *Electrolytic Shaping of Germanium and Silicon*, Bell System Technical Journal **35**, 333–347 (1956).
[12] Kuntyi, O., Zozulya, G., Shepida, M., *Porous silicon formation by electrochemical etching*, Adv. Mat. Sci. Eng. **2022**, 1482877 (2022).
[13] Calderón, A., Alvarado-Gil, J. J., Yu, G., Gurevich, A., Cruz-Orea, I., Delgadillo, Vargas, H., Miranda, L. C. M., Phys. Rev. Lett. **79**, 5022-5025 (1997).
[14] Hernández-Wong, J., Uriel Nogal, L., Rojas Marroquin, A., Luviano Elizalde, L., Rojas-Trigos, J. B., Marín Moares, E., Calderón, A., J. Appl. Phys. **137**, 085103 (2025).
[15] Yon, J. J., Barla, K., Herino, R., & Bomchil, G., J. Appl. Phys. **62**, 1042-1048 (1987).
[16] Carslaw, H. S. & Jaeger, J. C., *Conduction of Heat is Solids*, 2nd Ed., (Oxford Science Publications, New York, 1989).
[17] Mansanares, A. M., Bento, A. C., Vargas, H., Leite, N.F. & Miranda, L. C. M., Phys. Rev. **B 42**, 4477 (1990).
[18] Vargas, H. & L. C. M. Miranda, Phys. Rep. **161**, 43-101 (1988)
[19] Almond, D. P., Patel, P. M., *Photothermal Science and Techniques*, (Chapman & Hall, USA, 1996).
[20] Calderón, A., Muñoz-Hernández, R. A., Tomás, S. A., Cruz-Orea, A., Sánchez Sinencio, F., J. Appl. Phys. **84**, 6327-6329 (1998).